Japanese Journal of Applied Physics

New Inductively Coupled Plasma System Using Divided Antenna for Photoresist Ashing

To cite this article: Fujio Terai *et al* 2004 *Jpn. J. Appl. Phys.* **43** 6392

Japanese Journal of Applied Physics
Vol. 43, No. 9A, 2004, pp. 6392–6398

New Inductively Coupled Plasma System Using Divided Antenna for Photoresist Ashing

Fujio TERAI[1,2*], Hiroaki KOBAYASHI[2], Katsumi IYANAGI[2], Masashi YAMAGE[2],
Takao NAGATOMO[1] and Tetsuya HOMMA[1]

[1]*Postgraduate Course of Functional Control System, Shibaura Institute of Technology,*
3-9-14 Shibaura, Minato-ku, Tokyo 108-8548, Japan
[2]*Corporate Manufacturing Engineering Center, Toshiba Corporation,*
33 Shin-isogo-cho, Isogo-ku, Yokohama-shi, Kanagawa 235-0017, Japan

(Received December 10, 2003; accepted June 11, 2004; published September 9, 2004)

We have developed an inductively coupled plasma (ICP) system with a small chamber for 300-mm-diameter-wafer processes, and a good uniformity of ashing, and both low substrate temperature and low pressure were achieved. The features of this ICP system are substrate temperatures lower than 60°C in order to suppress chemical reactions, and low pressures of 3–5 Pa to suppress the both oxidation of Cu wiring and the degradation of low-*k* films. Furthermore, the antenna is divided plurally and capacitively coupled. This new antenna can achieve good uniformity in a small chamber because the capacitive coupling to the chamber through a quartz glass window can be easily controlled by reducing series impedance, even when the radio frequency (rf) power is very high. Moreover, the damage to the quartz glass window can be decreased by controlling the series impedance of the antenna, resulting in a long-lasting quartz window. The chamber structure was also optimized by performing an original plasma simulation to improve the uniformity of ashing rate. As results for 300-mm-diameter wafers in the 460-mm-diameter chamber, an average ashing rate of 848 nm/min with a uniformity of ±5.5% was obtained for photoresist films under the following conditions: an O_2 gas flow rate of 200 sccm, a substrate temperature of 60°C, a gas pressure of 3 Pa and an rf power of 4 kW. [DOI: 10.1143/JJAP.43.6392]

KEYWORDS: photoresist, ashing, plasma, ICP, antenna, uniformity, ashing rate

1. Introduction

In the latest technology for the fabrication of ultralarge-scale integrated circuits (ULSIs), a Cu wiring structure with a low-dielectric-constant (low-*k*) interlayer dielectric film has been used, in order to improve signal propagation speed and packing density.[1)] However, this Cu wiring structure has several problems caused by the low-*k*-film etching and photoresist ashing processes. One of the most serious problems is the degradation of the low-*k* dielectric film, resulting in an increase in dielectric constant. For the Cu wiring, the resistance of the wiring increases by oxidation due to heat formed during photoresist ashing. On the other hand, the wafer size has been increased from 200 mm to 300 mm in diameter to improve productivity. Although a conventional high-temperature ashing system can be used for the ashing of a photoresist on inorganic low-*k* films, there are problems such as the low heat resistance and low oxygen plasma tolerance of organic low-*k* films. Therefore, the selection of ashing systems and the refinement of the process are necessary for ashing a photoresist on organic low-*k* films. In siloxane-based organic low-*k* films, oxygen radicals dissociate CH_3 from low-*k* films, thereby which increasing dielectric constant and degrading via shape.[2)] The oxidation of the Cu film surface is also severe when the substrate temperature rises to 150°C, resulting in an increase in heat resistance.[3)] For this purpose, it is necessary to reduce electrically uncontrollable radical generation and to realize a high ashing rate using dominant ions under a low pressure. Therefore, inductively coupled plasma (ICP) was selected for high-density plasma generation at a low pressure.[4)] However, a capacitively coupled field is generated inside the chamber around the antenna in conventional ICP source equipment. This leads to the etching of the dielectric window and damages the inner wall of the chamber.[5–8)] Therefore, the conventional ICP system for mass production has a large-diameter chamber, and thick quartz windows, in order to separate the antenna from the chamber sidewall. An Al_2O_3 window was also used because it is more resistant to plasma damage than quartz windows.[9)] However, a window made of Al_2O_3 is expensive and is unsuitable for mass-production equipment. We proposed a new antenna divided plurally by capacitive coupling in order to reduce the high electric field of conventional ICPs. This new antenna can greatly decrease the amount of damage to the dielectric window. Furthermore, we have designed the chamber structure using an original plasma simulation, in order to enable its use for both low-*k*-film etching and photoresist ashing for a 300-mm-diameter wafer.

2. Experimental

2.1 *Design of ashing chamber*

In order to design a process chamber that enables the realization of uniform etching and ashing rates, the chamber structure was evaluated through experiments and simulations. The schematic diagram of the ICP photoresist ashing chamber used in these experiments is shown in Fig. 1. Gas plasma is generated with a 13.56 MHz rf power by inductive coupling with a divided antenna attached to the top of the process chamber. The rf power is well coupled through a quartz window 380 mm in diameter and 40 mm in thickness, which is located at the top of the process chamber. The wafer stage is equipped with an electrostatic chuck with a cooling system. The temperature of the wafer was maintained at 60°C. In order to optimize the chamber design parameters, such as the diameter of the reaction chamber, the diameter of the quartz window, the distance between the window and the wafer, and rf power, electron density was measured near the wafer surface using a plasma absorption probe[10)] and its relationship with photoresist ashing rate was investigated. These parameters govern the uniformity of etching and ashing rates. Experiments were conducted by

*E-mail address: fujio.terai@toshiba.co.jp

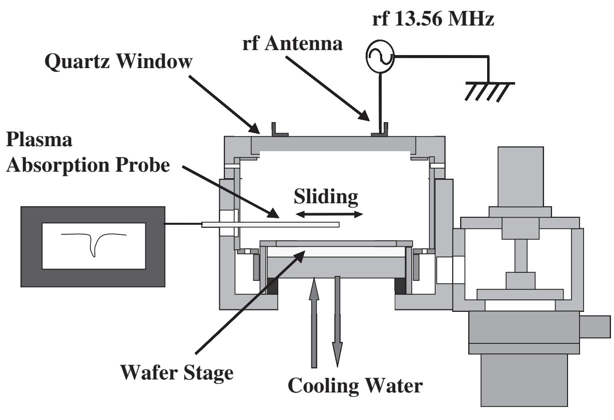

Fig. 1. Schematic diagram of ICP chamber.

setting the distance between the wafer and the quartz window at 145 mm, rf power at 1 kW and pressure at 0.6, 2.6 and 5.0 Pa. As shown in Fig. 2, electron density as a function of chamber radius is consistent with photoresist ashing rate. This result indicates that the uniformity of photoresist ashing rate can be predicted through the analysis of the uniformity of electron density for various chamber shapes. Therefore, the shape of the process chamber that enables the realization of uniform photoresist etching and ashing rates can be precisely evaluated using parameters such as the distance between the wafer and the quartz window, the diameter of the quartz window, rf power, and the simulated uniformity of electron density. The state of oxygen plasma was analyzed using the hybrid plasma equipment model (HPEM). Electromagnetic field is analyzed as a function of input power and chamber shape, and the dynamics of the electron are determined drawn by the Monte Carlo method, yielding the electronic energy distribution. Ionization rate and the number of dissociated ions are calculated using the database of electronic collision cross sections. As a result, the numbers of generated electrons and ions can be calculated. Based on the numbers of generated electrons and ions, a fluid model is used for the analyses of migration and diffusion due to an electric field, in order to elucidate the distribution of electron and ion densities.

2.2 *Reduction of capacitive coupling using the divided antenna*

In the ICP, there are capacitively coupled and inductively coupled components that are generated near the antenna. Although inductive coupling is effective for generating high-density plasma at a low pressure, the quartz window and the sidewalls of the chamber are attacked by ions induced by the electric field generated by capacitive coupling. If the voltage applied to the antenna is decreased, the component of capacitive coupling can be reduced. However, in this case, etching rate will be simultaneously reduced. Therefore, a plasma source that can control capacitive coupling and reduce damage to the quartz window was investigated. We found that by dividing the antenna and connecting the divided parts with each other capacitively, a decrease in etching rate can be avoided. In order to confirm the effect of the divided antenna, three types of antenna, nondivided, and divided into two and four, were prepared, and the etching properties were evaluated with an optical film thickness measurement system by examining a thermally grown silicon dioxide (SiO_2) film formed on a silicon (Si) wafer, which is attached to the vacuum side of the quartz window. The experimental conditions were an rf power of 1 kW, a pressure of 2 Pa, an oxygen gas flow rate of 90 sccm, a CF_4 gas flow rate of 10 sccm, and a wafer temperature of 60°C.

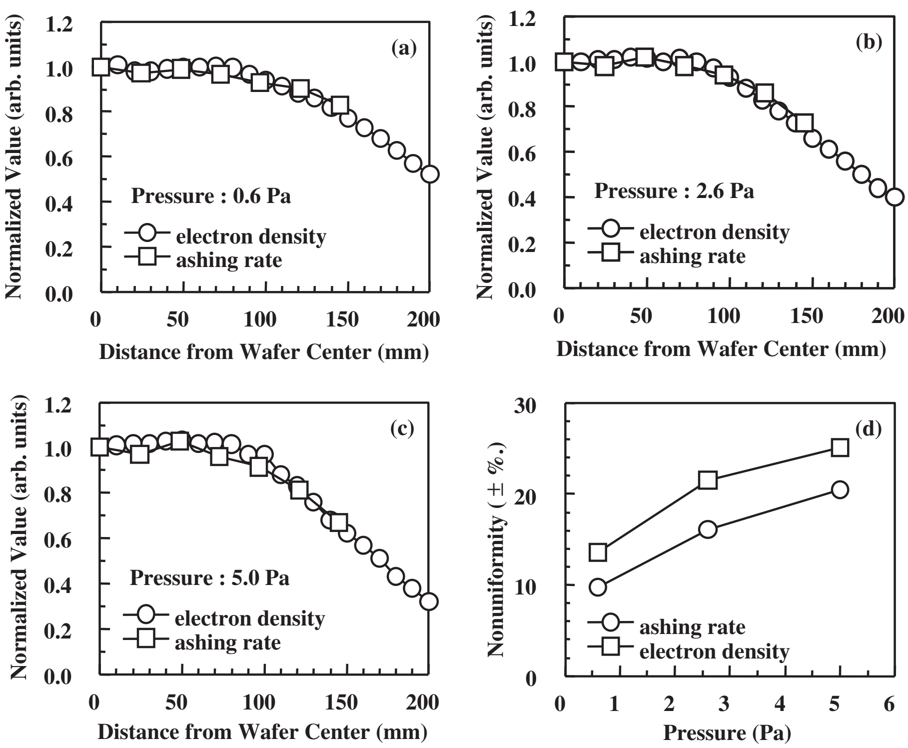

Fig. 2. Normalized ashing rate, electron density and nonuniformity, for chamber pressures of (a) 0.6, (b) 2.6 and (c) 5.0 Pa.

2.3 Ashing property of photoresist

In order to confirm the accuracy of the plasma simulation, a process chamber was prepared, where the diameter of the quartz window, the distance between the quartz window and the wafer, and rf power can be controlled. Ashing rate and in-plane uniformity were simulated under the following conditions: quartz window diameters of 380 mm and 430 mm, a distance between the quartz window and the wafer of 100–160 mm, an rf power of 1–4 kW, a pressure of 3 Pa, and a wafer temperature of 60°C. Since the electric potential of the wafer stage is set at 0 V, the energy due to ion impact is determined from the plasma electric potential. The plasma electric potential in ICP is generally approximately 20–30 V, and then the damage to the wafer can also be reduced. Photoresist film was formed on 300-mm-diameter wafers, and the change in thickness after the ashing process was measured with an optical film thickness meter.

3. Results and Discussion

3.1 Optimization of chamber shape

Figure 3 shows the electron density distribution determined by the simulation. A high-density area was observed directly below the antenna, and the density near the wafer was uniform. In order to improve the uniformity of ashing rate, it is necessary to make plasma density uniform above the wafer surface. Therefore, the chamber shape and process conditions must be optimized. The relationship between the chamber diameter and electron density distribution is shown in Fig. 4. When chamber diameter increases, the decrease in ashing rate at the wafer edge can be suppressed. However, a reduction in equipment size is required to enable mass production in a clean room. Therefore, it is necessary to improve the uniformity of ashing rate while reducing chamber diameter. Figure 5 shows the electron density along the radial direction 20 mm from the wafer, which was derived from the electron density distribution simulation as a function of the distance between the wafer and the quartz window. The conditions of the simulation were a constant pressure and an rf power of 3 Pa and 2.5 kW, respectively. When the distance was set at 160 mm, the ashing rate of the photoresist film at the wafer edge (near the sidewall of the chamber) decreased due to nonuniform plasma diffusion. When the distance was decreased to 100 mm, the effect of

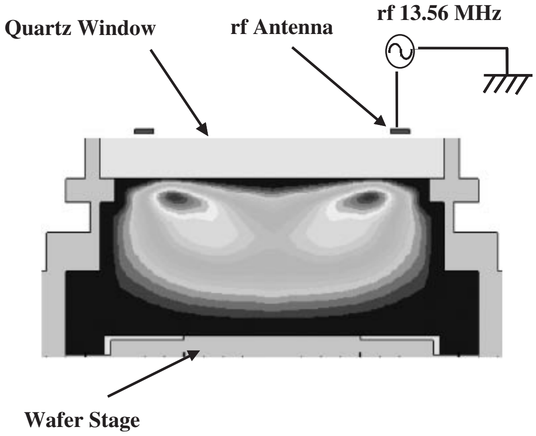

Fig. 3. Simulated electron density distribution.

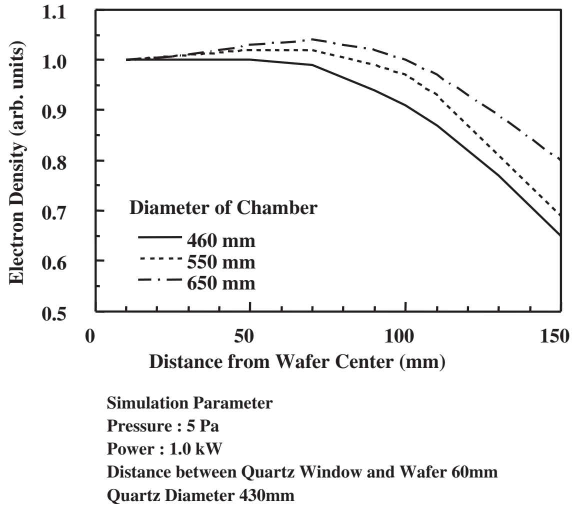

Fig. 4. Simulated electron density distribution as function of chamber diameter.

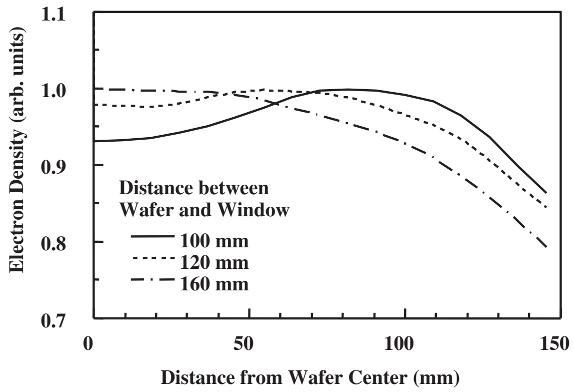

Fig. 5. Simulated electron density distribution as function of distance between wafer and quartz window.

plasma density at the ICP source was significant and plasma density consistently increased with change in antenna shape, thus the ashing rate at the center and wafer edge decreased. Therefore, the distance between the quartz window and the wafer must be optimized to achieve a high uniformity. Figure 6 shows the simulation results of the electron density distribution plotted against the diameter of the quartz window. The conditions of the simulation were again a constant pressure and an rf power of 3 Pa and 2.5 kW, respectively. We found that a large-diameter quartz window improves the uniformity of the ashing rate at the edge of the wafer. In this simulation, the antenna diameter was fixed, since the metal parts of the chamber supporting the quartz window stuck out of the chamber when the diameter of the quartz window was small, resulting in a difficul plasma diffusion. Figure 7 shows electron density distribution as a function of rf power. The conditions of the simulation were a distance between the quartz window and the wafer of 140 mm and a quartz window diameter of 380 mm. By increasing rf power, the decrease in ashing rate can be suppressed at the edge of the wafer, resulting in a high uniformity. On the basis of the above results, the distance between the quartz window and the wafer was selected to be

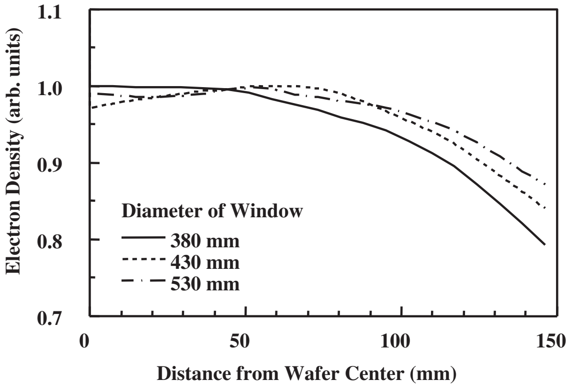

Fig. 6. Electron density distribution as function of diameter of quartz window.

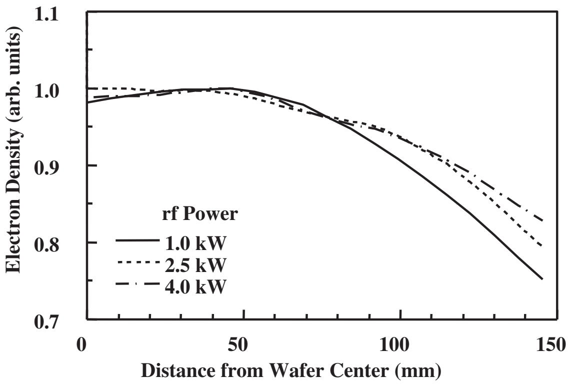

Fig. 7. Electron density distribution as function of rf power.

120 mm. It was clarified that a suitable distance between the quartz window and the wafer for obtaining ashing uniformity is 100 mm. However, the decrease in ashing rate at the center of the wafer cannot be suppressed by adjusting other parameters. On the other hand, the decrease in ashing rate at the edge can be suppressed by increasing the diameter of the quartz window and rf power. Therefore, the optimum distance of 140 mm was selected. As for the quartz window, uniformity can be improved by increasing its diameter. Since a small-diameter quartz window is preferred for achieving mechanical strength and suppressing the increase in equipment cost, a diameter of 430 mm was selected for the manufacturing equipment.

3.2 *Reduction of damage to quartz window*

Figure 8 shows the difference between the voltage applied to the nondivided antenna and to the antennas divided into two and four. Since the nondivided antenna is connected to the ground at the end terminal, the potential of the antenna becomes zero and decreased from the power input terminal at the matching box to the end terminal. For the antenna divided into two, since a condenser is inserted between the elements, an opposite polar potential due to the inductance of the antenna is generated by the inserted capacitance. Therefore, the potential generated due to the antenna inductance can be reduced to 1/4. Similarly, for the antenna divided into four, this potential can be reduced to 1/8. Moreover, the capacitance between elements was adjusted

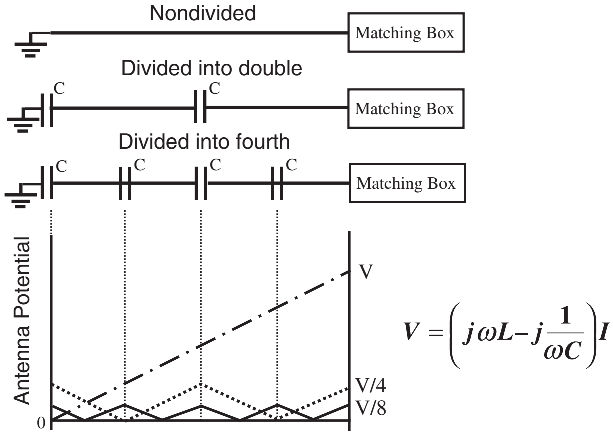

Fig. 8. Difference in voltage applied to nondivided antenna and antenna divided into two and four.

such that the voltage at the center of each element was minimum. Figure 9 shows the etching rate of the thermal SiO_2 film formed on the Si wafer attached to the quartz window, where the antenna was nondivided and divided into four. As for the nondivided antenna, the damage to the thermal SiO_2 film close to the matching box is significant, where the plasma potential is high. However, for the antenna divided into four, the plasma potential difference between positions is small, and the damage is uniform. Figure 10 shows the damage to the quartz window caused by the voltage applied to the nondivided antenna, and the antennas divided into two and four. Since quartz is used for the window, the evaluation was conducted, using a thermal SiO_2 film formed on a Si wafer and attached to the quartz window at the antenna position, by calculating etching rate using CF_4/O_2 gas plasma. The etching rate was reduced from 19.1 nm/min for the nondivided antenna to 6.2 nm/min for the antenna divided into four, indicating a three times longer life.

3.3 *Ashing property of photoresist*

It is considered that the plasma density along the divided antenna becomes uniform, as shown in Fig. 9. Therefore, uniform ashing was also expected as an effect of the divided antenna. However, as shown in Fig. 11, the uniformity of ashing rate was not improved. This is because the radicals diffused in the chamber, due to the large distance (150 mm) between the quartz window and wafer. Figure 12 shows the distribution of ashing rate and its nonuniformity for the photoresist film when the diameter of the quartz window is changed from 380 mm to 430 mm. The in-plane distribution consistently improved with the simulation results when the quartz window was enlarged. Also, the ashing rate at the edge of the wafer improved, as did the nonuniformity. Figure 13 shows the film thickness measurement points excluding 5 mm from the wafer edge. From the data measured at 61 points, nonuniformity was calculated

$$\text{Nonuniformity} = (\text{Max} - \text{Min})/(\text{Max} + \text{Min}) \times 100. \quad (1)$$

Ashing rate was obtained from the average of the data measured at the 61 points. Figure 14 shows the distribution of ashing rate and its nonuniformity when the distance between the quartz window and the wafer was changed from

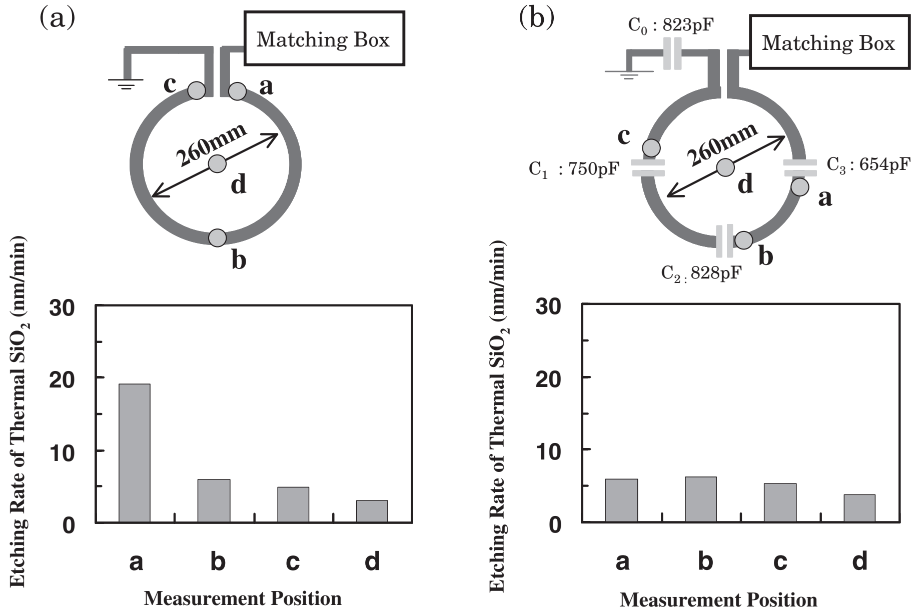

Fig. 9. Etching rate of thermal SiO_2 film attached to quartz window for (a) nondivided antenna and (b) antenna divided into four.

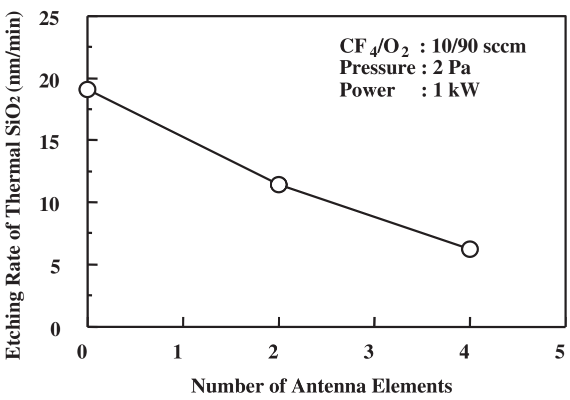

Fig. 10. Etching rate of thermal SiO_2 film attached to quartz window, plotted against applied voltage to nondivided antenna and an antenna divided into two and four.

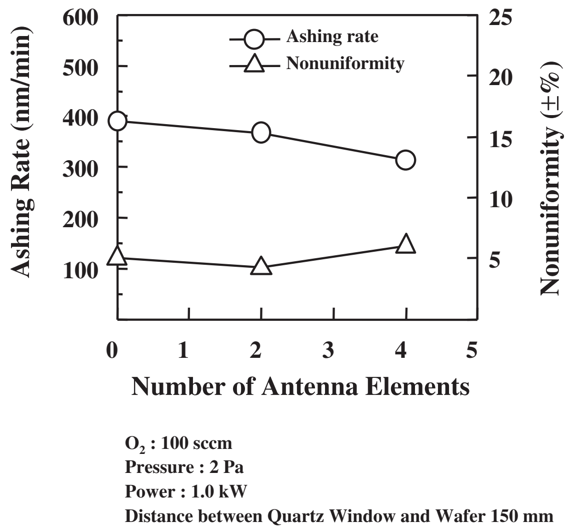

Fig. 11. Ashing rate and its nonuniformity for nondivided antenna, and antenna divided into two and four.

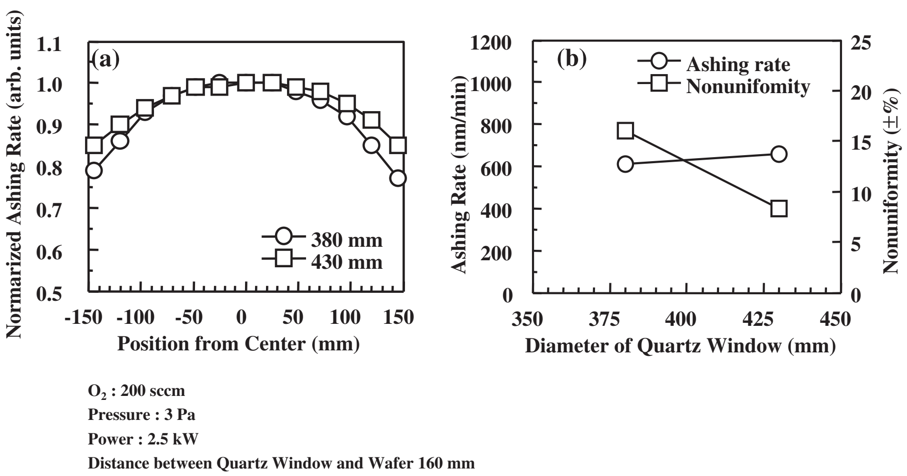

Fig. 12. Distribution of ashing rate and its nonuniform quartz window diameters of 380 and 430 mm. (a) and (b) show ashing rates for diameters of 380 and 430 mm, respectively, and non-uniformity.

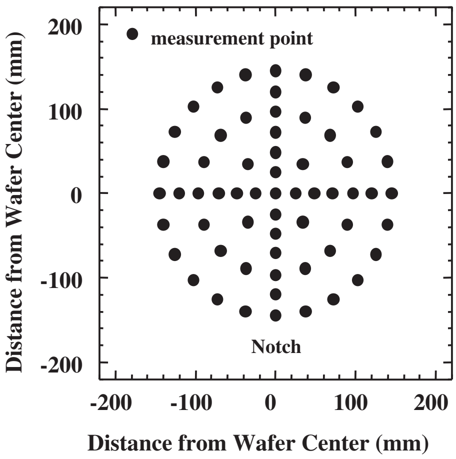

Fig. 13. Measurement points for film thickness on 300-mm-diameter Si wafer.

100 to 160 mm. The distribution of ashing rate was obtained from the ashing rates on the *x*-axis including the wafer center. This result was also consistent with the simulation results. Although the nonuniformity improved, the ashing rate at the center of the wafer was reduced. Figure 15 shows the distribution of ashing rate and its nonuniformity, for rf power changed from 1 to 4 kW. This result is also consistent with the simulation results, indicating that the ashing rate at the edge of the wafer increases and its nonuniformity improves with increasing rf power.

4. Conclusions

A plasma source in which an rf antenna is divided and connected to condensers was developed and the problematic capacitive coupling of the ICP system was reduced. This improvement resulted in the high efficiency of the plasma, the reduction of damage to the quartz window and increased productivity. Therefore, it became possible to increase the input power to the antenna, and then the uniformity of ashing rate was also improved for the chamber with a small diameter. In order to optimize this plasma source for etching and ashing equipment that can handle a 300-mm-diameter wafer, the optimum chamber shape was determined through the simulation of the plasma state. The calculation of electron density distribution according to chamber shape enabled the estimation of the ashing rate distribution, so that an ICP source with a high uniformity could be developed. The optimum parameters of the chamber design are a chamber diameter of 460 mm, a quartz window diameter of 430 mm, a distance between the quartz window and the wafer of 140 mm, and an rf power of 4 kW. For 300-mm-

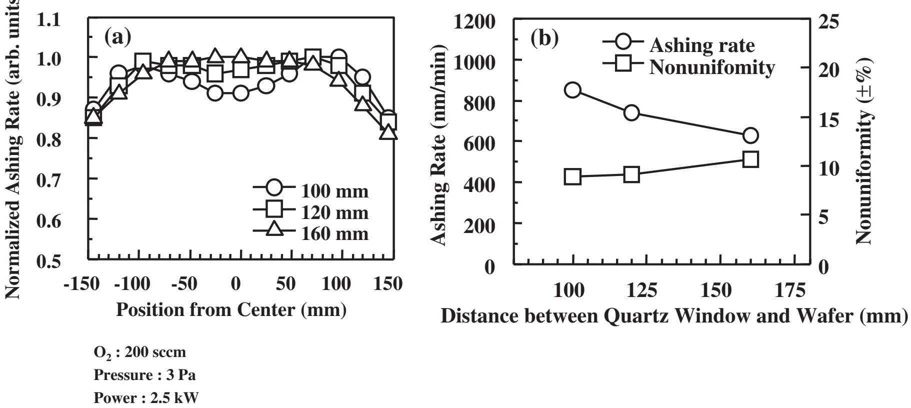

Fig. 14. Distribution of ashing rate and its nonuniformity for various distances between quartz window and wafer. (a) and (b) shows ashing rate for a distance between quartz window and wafer of 100 to 160 mm, and nonuniformity, respectively.

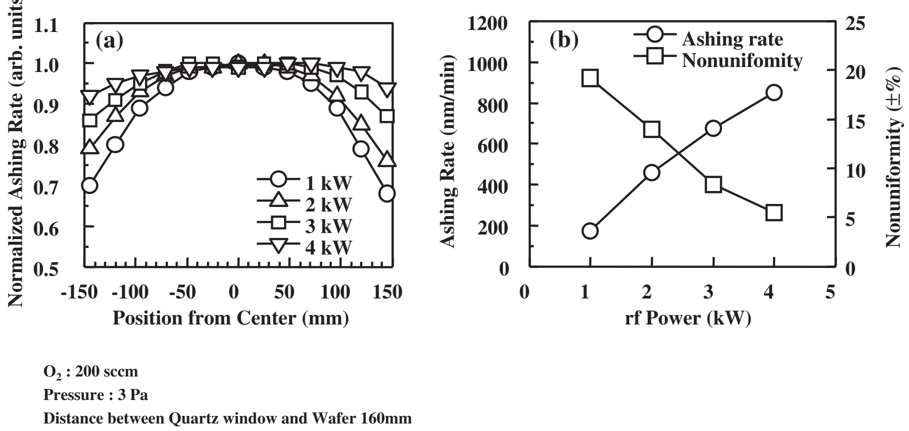

Fig. 15. Distribution of ashing rate and its nonuniformity when the rf power was changed. (a) and (b) shows the ashing rate for rf power changed from 1 to 4 kW, and nonuniformity, respectively.

diameter wafers, the average ashing rate of 848 nm/min with a nonuniformity of ±5.5% was achieved for photoresist films under the following conditions: an O_2 gas flow rate of 200 sccm, a substrate temperature of 60°C, a gas pressure of 3 Pa and an rf power of 4 kW.

Acknowledgments

The authors are very grateful to Dr. Y. Kataoka, Dr. M. Kanoh, and Mr. H. Ita for their encouragement and helpful discussion.

1) C. Janowiak, S. Ellingboe and I. Morey: J. Vac. Sci. Technol. A **18** (2000) 1859.
2) H. Nagai, Y. Maeda, M. Hiramatsu, M. Hori and T. Goto: 2001 Dry Process Int. Symp., p. 147.
3) A. Kojima, T. Sakai and T. Ohiwa: 2001 Dry Process Int. Symp., p. 165.
4) J. Hopwood: Plasma Sources Sci. Technol. **1** (1992) 109.
5) H. Sugai, K. Nakamura and K. Suzuki: Jpn. J. Appl. Phys. **33** (1994) 2189.
6) Y. Hikosaka, M. Nakamura and H. Sugai: J. Appl. Phys. **33** (1994) 2157.
7) N. Jiwari, H. Iwasawa, A. Narai, H. Sakaue, H. Shindo, T. Shoji and Y. Horiike: Jpn. J. Appl. Phys. **32** (1993) 3019.
8) Z. Yu and D. Shaw: J. Vac. Sci. Technol. A **13** (1995) 871.
9) K. Yoshida, H. Miyamoto, E. Ikawa and Y. Murao: Jpn. J. Appl. Phys. **34** (1995) 2089.
10) H. Kokura, K. Nakamura, I. P. Ghanashev and H. Sugai: Jpn. J. Appl. Phys. **38** (1999) 5262.